



HHS Public Access

Author manuscript

Laryngoscope. Author manuscript; available in PMC 2021 October 26.

Published in final edited form as:

Laryngoscope. 2013 December ; 123(12): E109–E115. doi:10.1002/lary.24174.

Mouse Cochleostomy: A Minimally Invasive Dorsal Approach for Modeling Cochlear Implantation

Hakan Soken, MD,

Department of Otolaryngology Head and Neck Surgery, University of Iowa, Iowa City, Iowa, U.S.A.

Barbara K. Robinson, MS,

Department of Otolaryngology Head and Neck Surgery, University of Iowa, Iowa City, Iowa, U.S.A.

Shawn S. Goodman, PhD,

Department of Communication Sciences and Disorders, University of Iowa, Iowa City, Iowa, U.S.A.

Paul J. Abbas, PhD,

Department of Otolaryngology Head and Neck Surgery, University of Iowa, Iowa City, Iowa, U.S.A.

Department of Communication Sciences and Disorders University of Iowa, Iowa City, Iowa, U.S.A.

Marlan R. Hansen, MD,

Department of Otolaryngology Head and Neck Surgery, University of Iowa, Iowa City, Iowa, U.S.A.

Jonathan C. Kopelovich, MD

Department of Otolaryngology Head and Neck Surgery, University of Iowa, Iowa City, Iowa, U.S.A.

Abstract

Objectives/Hypothesis: The murine model has been used extensively to model and study human deafness. Technical difficulty in the surgical approach due to the small size of the tympanic bulla and a robust stapedial artery has limited its application for studies of cochlear implantation and electrical stimulation. We describe a minimally traumatic, stapedial artery–sparing approach to the round window that may be used to access the mouse cochlea for acute or chronic studies of implantation and stimulation.

Study Design: Animal model.

Send correspondence to Marlan R. Hansen, MD, 200 Hawkins Dr, 21163 PFP, Iowa City, IA, 52242-1078., marlan-hansen@uiowa.edu.

Hakan Soken, MD's present affiliation is Department of Otolaryngology, Eskisehir Military Hospital, Eskisehir, Turkey.

Additional Supporting Information may be found in the online version of this article.

The authors have no other funding, financial relationships, or conflicts of interest to disclose.

Methods: Fifteen C57BL6J mice were used to validate this approach. Auditory brainstem response threshold and distortion product otoacoustic emissions were obtained preoperatively and 2 weeks postoperatively to determine hearing preservation results.

Results: The approach provided excellent exposure for round-window implantation. Substantial hearing was preserved in all animals with a mean postimplantation auditory brainstem response threshold increase of 27.8 dB. Otoacoustic emissions were lost in subjects with the largest threshold shifts.

Conclusions: Residual hearing after cochlear implantation is a determinant of success both with standard cochlear implant electrodes and with electrodes designed to optimize hearing preservation. Here, we have preserved usable hearing after implantation of C57BL6J mice, an endogenous model of human presbycusis. The murine model may become a powerful tool to assay the effects of cochlear intervention in different genetic backgrounds.

Keywords

Cochlear implant; mouse; acoustic evoked auditory brainstem response; distortion product otoacoustic emissions; stapedia artery; hearing preservation

INTRODUCTION

Experimental research in otology has traditionally employed several mammalian models (i.e., rats, mice, guinea pigs) because of their availability and anatomic similarity to the human ear. Among these species, mice afford many advantages for *in vivo* research, including availability, size, low cost, ease of handling, and increased housing density. Mice have short gestation times and life-spans, such that the effects of age and interventions are apparent in a shorter time frame.

Perhaps the most important advantage in using the mouse for biomedical research is the ability to experimentally manipulate the mouse genome. The transgenic mouse was first described in 1980.¹ Since then, advances in this area have been dramatic, enhanced by the availability of the mouse genome,² the ability to conditionally knock out genes in specific target tissues,³ and the capacity to replace mouse genes with genes that encode reporter proteins.⁴ Recently, with the increasing availability of spontaneous and transgenic mutant mouse lines and extensive data to indicate that human hearing loss is accurately modeled in the mouse,^{5,6} the mouse has become a model of choice for deafness research. The C57BL/6J mouse, specifically, has been validated as a model for age-related hearing loss that does not require the use of noise or ototoxins in that cochleae develop large outer hair cell lesions and then inner hair cell lesions that spread from base to apex, starting at 3 months of age.⁷

Although mice provide substantial advantages over other animal models, rats, guinea pigs, and cats have dominated the field of cochlear implant research. This is due in part to the considerable size of their tympanic bulla (TB) (i.e., temporal bulla), permitting easy access to the inner ear.^{8,9} Thus, resources describing surgical anatomy of the rodent cochlea are mostly limited to rat and guinea pigs.¹⁰⁻¹² Pinilla et al. describe simple ventral surgical access to the rat's middle ear causing minimal morbidity and mortality to the animals,¹³ and Jero et al. report a similar approach in the mouse.¹⁴ With specific reference to cochlear

implantation (CI), Lu and Shepherd presented a dorsal surgical approach cauterizing the stapedia artery (SA) and then performing a round window (RW) cochleostomy that was described as safe and effective for acute and chronic electrical stimulation of the auditory nerve in the rat model.¹⁵

The primary technical obstacles to CI in mice are diminished size and the SA. In humans, the SA regresses in the third month of prenatal life; in rare cases the SA remains persistent¹⁶ and may cause bleeding if unexpectedly encountered during surgery. In a number of rodents including rats, mice, and gerbils, however, the SA persists throughout life.¹⁷ With conventional ventral approaches to the bulla, the SA partially or completely obstructs exposure to the RW. In the case of obstruction, the SA must be sacrificed or the approach changed by expanding the surgical defect of the bulla. This additional trauma is especially detrimental in attempts to model hearing preservation CI in rodents. We therefore sought to develop a new minimally traumatic surgical approach for CI in mice to provide access to the scala tympani while sparing the SA. This report describes a dorsal approach to the mouse cochlea that minimizes surgical trauma, morbidity, and mortality while adequately preserving hearing.

MATERIALS AND METHODS

Animals and Groups

Eighteen C57BL/6J mice were used in this study, comprised of 10 males and eight females ranging in weight from 16 to 28 g and in age from 44 to 56 days. Animals were unilaterally implanted with a platinum-iridium wire (0.005 inch) placed in the scala tympani via a modified, minimally invasive dorsal approach as detailed later. In each of these, the contralateral ear was used as a nonoperative control for physiologic testing. The Institutional Animal Care and Use Committee of the University of Iowa approved all procedures.

Physiologic Tests

The hearing status of each animal was assessed using click auditory brainstem response (ABR) and distortion product otoacoustic emissions (DPOAEs) both before surgery and 2 weeks postoperatively.

ABRs and DPOAEs were measured using an Etymotic Research ER10B1 probe microphone (Elk Grove, IL) coupled to two Tucker Davis Technologies MF1 Multi-Field Magnetic Speakers (Alachua, FL). Stimulus presentation and recording were controlled using custom software running on a PC connected to a 24-bit external sound card (Motu UltraLite mk3).

A custom-built differential amplifier with a gain of 1,000 dB amplified acoustic ABR responses. The output was passed through 6-pole Butterworth high-pass (100 Hz) and low-pass (3 kHz) filters and then to a 16-bit analog-to-digital converter (100,000 samples/s). Responses were recorded using standard signal-averaging techniques. Typically, 500 to 2,000 sweeps were used in each averaged response, depending on signal-to-noise conditions as determined by the experimenter.

DPOAEs were measured using frequency glides rather than the standard paradigm of testing one frequency at a time. The glide method is faster than the standard method, yields comparable results in terms of DPOAE magnitude, and allows variable, finely spaced frequency analysis. Stimuli consisted of linear frequency glides from 1 to 18 kHz, changing at a rate of approximately 5.7 kHz/s (3 seconds per sweep). The primary frequency glides f_1 and f_2 had a constant frequency ratio of $f_2/f_1 = 1.22$. The levels of the primaries were fixed at 65 dB SPL and 55 dB SPL for f_1 and f_2 , respectively. An in situ level calibration was performed before each measurement, and the levels of the electrical stimulus drives were adjusted to create a flat acoustic amplitude response at the calibrated probe microphone. Standing waves were not expected to affect the measurements, because the distance between the inlet of the probe microphone and the eardrum was approximately 0.3 cm, effectively placing the highest quarter-wavelength null at a frequency >18 kHz.

Recorded waveforms were bandpass filtered (0.8–18.2 kHz) using a finite impulse-response filter. Filter group delay (30 milliseconds) was corrected for. Each measurement consisted of the bi-squares-weighted average of 15 stimulus presentations. This method controlled artifact by down-weighting noisy samples in the recorded waveforms. The cubic distortion products and associated noise floors were extracted by a custom-designed digital heterodyne filtering operation. Two noise floor calculations (1/12th octave above and below the cubic distortion frequency) were averaged to give a single noise floor estimate.

Data and Statistical Analysis

ABR and DPOAE threshold data were recorded and managed using Excel software (Microsoft, Redmond, WA). Differences in mean ABR thresholds were tested for statistical significance using a one-way analysis of variance (ANOVA) with post hoc Kruskal-Wallis analysis using SigmaStat software (Ashburn, VA).

Surgical Procedure

The study involved the use of an operating microscope (M220 F12; Leica, Buffalo Grove, IL) with a digital camera and recording system (Leica MDRS3) adapted to the surgical microscope; illustrations are drawn according to the images obtained. Video footage is provided as an online addendum. Mice are anesthetized with ketamine (100 mg/kg, intraperitoneal) and xylazine (10 mg/kg, intraperitoneal). Once anesthetized, body temperature is maintained with a sterile wrapped circulating warm-water heating pad.

The mouse is positioned prone on the surgical table to optimize respiratory functions (Fig. 1A). The animal can later be repositioned for better exposure. Povidone iodine surgical scrubs are applied to disinfect the skin. A local anesthetic (Lidocaine HCl 1% and epinephrine 1:100,000) is infiltrated into a 10- to 12-mm postauricular incision line extending ventrally through the mandibular angle (Fig. 1B). The mouse is then draped with a 20 × 15-cm sterile surgical towel with a 15-mm kite-shaped hole placed over the surgical site. Following incision and blunt dissection of superficial fascia of the neck, the greater auricular nerve is identified as it crosses rostrocaudally over the sternocleidomastoid muscle (SCM) and cut (Fig. 2A and 2B). The superficial fascial layers of the neck are further dissected to identify the facial nerve (CN VII). The SCM and anterior scalene muscles are

either cut proximally or retracted dorsocaudally using a tie-back stitch. The posterior belly of the digastric muscle (PBD), arising from the dorsocaudal part of the TB ventrocaudal to the trunk of CN VII (Fig. 2C and 2D), is dissected from the TB using bipolar electrocautery. A bony ridge of the TB lies rostrocaudally under the insertion of the PBD. The anterior edge of the splenius capitis muscle may be incised over the CN VII trunk.

To standardize the placement of the tympanotomy for minimally traumatic access to the tympanum in the vicinity of the RW, it is placed in a triangle-shaped area created by drawing lines on three key landmarks: 1) the digastric ridge, 2) the tympanomastoid fissure, 3) the line joining the two by crossing the external orifice of the CN VII (stylomastoid foramen) (Fig. 3A–3D).

Before drilling, the site of the bulla should be cleared of fibromuscular tissue to prevent injury to neighboring tissues (CN VII, etc.). Creation of the tympanotomy is begun in the dorsocaudal portion of the triangle using a 0.7-mm diamond burr. This position allows a straight path into the basal turn of the cochlea through the RW (Fig. 4D). Drilling is done at a slow speed for prevention of SA injury after the tympanotomy. If the tympanic mucosa is still intact, microforceps are used to penetrate the final layer. With our preparation, the SA lies at the far inferior border of the tympanotomy, and care is taken to avoid injury. At this point, the animal is rolled slightly away from the operator to facilitate visualization of the inferior margin of the RW (Fig. 4A and 4B). The bony cap of the bulla overlying the RW is carefully thinned using a 0.5-mm diamond burr, pausing to remove fine bone chips with microforceps as necessary, until the superior margin of the RW is clearly visible (Fig. 4C).

Immediately before RW membrane penetration, a 1 × 1mm graft of trapezius fascia is removed and placed on the surgical site. The membrane of the RW is perforated using a 0.005-inch platinum-iridium wire to open the scala tympani. This is inserted without resistance to a depth sufficient to keep it from extruding (≈ 1.5 –2 mm). To minimize leaking of perilymphatic fluid, the length of time the cochlea remains exposed should be minimized. Once the cochlea is opened and implant placed, the fascia graft is packed gently and deeply into the tympanotomy hole, thus sealing the cochleostomy site. To prevent conductive hearing loss and preserve residual hearing, care is taken not to pack the fascia graft rostrally through the epitympanum. The SCM and anterior scalene muscle should be loosely reapproximated, followed by skin and soft-tissue closure.

RESULTS

Fifteen of 18 animals (83%) survived. Total operative time ranged from 30 to 45 minutes. Intraoperative SA bleeding was the cause of death in one instance. Two animals expired from respiratory depression secondary to depth of anesthesia. Facial nerve injury was not noted in any animals. On otomicroscopy, middle ear fluid was noted in two of the 15 animals at 2 weeks postoperatively.

ABR Results

Figure 5A and 5B display examples of recordings of preoperative and 2-week postsurgery ABR, respectively. In the 15 surviving animals, change in ABR threshold ranged from –3 to

60 dB, with an average threshold shift of 27.8 ± 5 dB (Fig. 5C). In contralateral ears, change in ABR threshold ranged from -9 to 9 dB, with an average threshold shift of 0.6 ± 1 dB. The difference between the mean postoperative ABR threshold was statistically significant compared to the mean preoperative threshold and the mean threshold of the contralateral ear ($P < .01$, ANOVA).

DPOAE Results

Responses above the noise floor were deemed to be reliable up to 18 kHz, or midfrequency hearing for C57B16J mice. In situ calibrations and noise floors were checked for each measurement and found to be stable and comparable across all conditions. Figure 6 presents DPOAE results. Postoperative results were comparable to preoperative for the nonoperated ear (mean shift at $f_2 = 18$ kHz of 0.2 ± 2.4 dB). Preoperative DPOAE revealed variability in the test ears for this subject cohort. Postoperative retesting (2 weeks) in the test ear revealed a drop in hearing across the entire frequency range, with the lower frequencies falling into the noise floor. At 18 kHz, nine of 15 animals had responses above the noise floor (>6 dB signal to noise ratio) at the postoperative retest. For these nine animals, the average postoperative shift was -12.2 ± 12.3 dB. The range of shifts was 4.0 to -31.8 dB.

For subjects that had measureable postoperative DPOAE responses in the test ear at f_2 of 18 kHz or below ($n = 9$), ABR threshold shift was 15.7 ± 3.3 dB. For subjects that had no responses, ABR threshold shift was 51 ± 3.7 dB.

DISCUSSION

The mouse cochlea is located on the medial wall of the bulla and contains only 1.5 full turns compared to 2.5 to 2.75 in humans and 4.25 in guinea pigs.¹⁸ In mice, the presence of the SA severely restricts surgical access to the cochlea through the RW. It runs along the base of the cochlea and through the crura of the stapes. Lu and Shepherd described successful cauterization of the SA to provide sufficient access to the RW in the rat.¹⁵ They showed that cauterizing the SA did not affect the hearing status in the frequency range 0.5 to 16 kHz. Emadi et al. also reported no significant hearing loss in gerbils using compound action potential thresholds over a frequency range of 1.6 to 50 kHz following removal of the SA.¹⁹ However, others have argued that the artery should be preserved to preserve hearing or even survival of the animal.^{20,21} We felt that development of an approach that preserves the SA in mice would be ideal because the murine cochlea is more susceptible to hearing loss than in other species. Furthermore, attempts to cauterize the SA can itself increase risk of bleeding and iatrogenic trauma. Finally, attempts to model hearing preservation implantation require minimizing intracochlear transfer of thermal and vibratory energy.

The primary disadvantage of the dorsal approach to the cochlea in the mouse is increased likelihood of CN VII injury. The facial nerve is small, superficial, and antero-rostral in position. Hemifacial paralysis may adversely affect the animal's nutrition and general health. In our dorsal approach, because the tympanotomy is near the CN VII trunk, the nerve can be injured by direct mechanical disruption from a rotating burr, by indirect injury due to wrapping fascial layers overlying CN VII around the rotating burr, or via injudicious use of electrocautery. Nerve injuries due to surgical technique often result from thermal injury

by using monopolar electrocautery or traction of the nerve. Bipolar electrocautery is thus preferred for preventing thermal injury.

In addition to basic surgical measures (e.g., hemostasis, maintenance of body temperature and fluid status, close observation of vital functions) the surgical position of the animal is one of the most important issues for survival surgery. The animal's respiratory function should not be compromised by overextension of forelegs or excessive body tilt that causes pressure from the abdominal organs on the diaphragm. Inappropriate body position of the animal is also a potential risk for aspiration of the tracheobronchial secretions. The normal body posture of the mouse is the prone position, which is optimal for respiratory function. Several advantages of the ventral approach have been described, including quick surgical access and reduced risk of facial nerve injury; however, the animal is placed in supine position throughout the surgery. Thus for CI experiments that require prolonged anesthesia coupled with long-term survival, we find a dorsal approach with prone position of the animal to be preferable.

The propensity to develop a persistent middle ear effusion due to surgical trauma represents a disadvantage of the conventional postauricular approaches used extensively in rodent surgery. This can be troublesome if inner ear manipulations and physiologic tests are planned. We therefore modified our approach to minimize middle ear manipulation and trauma. These modifications were critical to reducing middle ear effusion such that gross effusion was noted in only two animals on otomicroscopy. Still, based on the loss of DPOAEs in subjects with the highest threshold shifts, it is reasonable to assume that residual middle ear fluid may have contributed to hearing loss in these instances.

The murine model is a workhorse of deafness and hearing loss research in part due to the natural propensity for rapid development of cochlear pathology consistent with presbycusis in certain strains. Despite this advantage, applications of the mouse model in CI research have been limited due to technical challenges. Recent advances in minimally traumatic insertion and hybrid short electrode arrays have been successful in capitalizing on useful residual low-frequency hearing in cochlear implantees and have broadened the patient population that may be helped by CI.²² Preservation of residual hearing after implantation is of paramount concern in this presbycusis patient population. Animal studies of the effect of electrical stimulation on acoustic response parameters, that is, eighth nerve compound action potentials, have noted a significant difference between normal hearing and presbycusis animals,²³ demonstrating the importance of appropriately modeling these interactions. Novel animal models of hearing preservation CI have been recently described using excitotoxic noise damage to mimic human presbycusis in Mongolian gerbils.²⁴ Postimplantation click ABRs revealed hearing loss ranging from 0 to 60 dB, with the majority of subjects retaining selective responses to low-frequency tone pips. These data are consistent with our model.

Our data suggest that middle ear effects may be an important confound in the mouse model of implantation even when not identified on otoscopy. Here, ABR threshold shift was disproportionately large in ears in which otoacoustic emissions were below the noise floor postoperatively (51 vs. 16 dB). Therefore, initial preservation of otoacoustic emissions may be a critical screen to adequately model hearing preservation implantation. Ultimately the

mouse model offers the opportunity to study the effect of implantation and chronic electrical stimulation on intrinsically susceptible cochleae analogous to those of our patients while avoiding potential confounds such as extensive ototoxin or noise exposure.

CONCLUSION

As the mouse is rapidly becoming the mammalian model of choice for investigations of the inner ear due to the experimental power provided by mouse genetic techniques, it is important to develop surgical approaches that facilitate implantation and stimulation of the mouse cochlea while preserving remaining cochlear function. Here we describe a modified dorsal approach to the mouse cochlea through the RW that is easy, fast, reliable and associated with minimal morbidity and mortality. In our hands, it is favored over other approaches for long-term experiments that require direct access to the cochlea and RW, particularly those that require hearing preservation.

Supplementary Material

Refer to Web version on PubMed Central for supplementary material.

ACKNOWLEDGMENTS

The authors are grateful to Kay Klein for her assistance with video editing.

This study was supported by NIH T32 DC000040 grant as well as NIDCD-P30 DC 010362.

BIBLIOGRAPHY

1. Gordon JW, Scangos GA, Plotkin DJ, Barbosa JS, Ruddle FH. Genetic transformation of mouse embryos by microinjection of purified DNA. *Proc Natl Acad Sci USA* 1980;77:7380–7384. [PubMed: 6261253]
2. Mouse Genome Sequencing Consortium et al. Initial sequencing and comparative analysis of the mouse genome. *Nature* 2002;420:520–562. [PubMed: 12466850]
3. Kuhn R, Schwenk F, Aguet M, Rajewsky K. Inducible gene targeting in mice. *Science* 1995;269:1427–1429. [PubMed: 7660125]
4. Lois C, Hong EJ, Pease S, Brown EJ, Baltimore D. Germline transmission and tissue-specific expression of transgenes delivered by lentiviral vectors. *Science* 2002;295:868–872. [PubMed: 11786607]
5. Avraham KB, Hasson T, Steel KP, et al. The mouse Snell's waltzer deafness gene encodes an unconventional myosin required for structural integrity of inner ear hair cells. *Nat Genet* 1995;11:369–375. [PubMed: 7493015]
6. Friedman TB, Schultz JM, Ben-Yosef T, et al. Recent advances in the understanding of syndromic forms of hearing loss. *Ear Hear* 2003;24:289–302. [PubMed: 12923420]
7. Spongr VP, Flood DG, Frisina RD, Salvi RJ. Quantitative measures of hair cell loss in CBA and C57BL/6 mice throughout their life spans. *J Acoust Soc Am* 1997;101:3546–3553. [PubMed: 9193043]
8. Goksu N, Hazirolu R, Kemaloglu Y, Karademir N, Bayramoglu I, Akyiliz N. Anatomy of the guinea pig temporal bone. *Ann Otol Rhinol Laryngol* 1992;101:699–704. [PubMed: 1497279]
9. Suzaki Y, Wada H, Oyama K, Koboyashi T, Houzawa K, Tanaka T. Dynamic behavior of the guinea pig middle ear [in Japanese]. *Nihon Jibiinkoka Gakkai Kaiho* 1997;3:342–350.
10. Hellstrom S, Salen B, Stenfors LE. Anatomy of the rat middle ear, a study under the dissection microscope. *Acta Anat* 1982;112:346–352. [PubMed: 7113638]

11. Wysocki J. Topographical anatomy of the guinea pig temporal bone. *Hear Res* 2005;199:103–110. [PubMed: 15574304]
12. Judkins RF, Li H. Surgical anatomy of the rat middle ear. *Otolaryngol Head Neck Surg* 1997;117:438–447. [PubMed: 9374164]
13. Pinilla M, Ramirez-Camacho R, Jorge E, Trinidad A, Vergara J. Ventral approach to the rat middle ear for otologic research. *Otolaryngol Head Neck Surg* 2001;124:515–517. [PubMed: 11337654]
14. Jero J, Tsen CJ, Mhatre AN, Lalwani AK. A surgical approach appropriate for targeted cochlear gene therapy in the mouse. *Hear Res* 2001;151:106–114. [PubMed: 11124456]
15. Lu W, Xu J, Shepherd RK. Cochlear implantation in rats: a new surgical approach. *Hear Res* 2005;205:115–122. [PubMed: 15953521]
16. Thiers AT, Sakai O, Poe DS, Curtin HD. Persistent stapedial artery: CT findings. *Am J Neuroradiol* 2000;21:1551–1554. [PubMed: 11003295]
17. Ortug C. A study on the rat stapedial artery under the dissection microscope. *Turk J Med Sci* 2001;31:117–119.
18. Kucuk B, Kazuhiro A. Microanatomy of the mouse osseous cochlea: a scanning electron microscopic study. *Arch Histol Cytol* 1989;52:173–182. [PubMed: 2505821]
19. Emadi G, Richter CP, Dallos P. Stiffness of the gerbil basilar membrane: radial and longitudinal variations. *J Neurophysiol* 2004;91:474–488. [PubMed: 14523077]
20. Preatorius M, Limberger A, Muller M, et al. A novel microperfusion system for the long-term local supply of drugs to the inner ear: implantation and function in the rat model. *Audiol Neurootol* 2001;6:250–258. [PubMed: 11729327]
21. Yamamoto H, Tominaga M, Sone M, Nakashima T. Contribution of stapedial artery to blood flow in the cochlea and its surrounding bone. *Hear Res* 2003;186:69–74. [PubMed: 14644460]
22. Gantz BJ, Hansen MR, Turner CW, Oleson JJ, Reiss LA, Parkinson AJ. Hybrid 10 clinical trial: preliminary results. *Audiol Neurootol* 2009;14(suppl 1):32–38.
23. Stronks HC, Versnel H, Prijs VF, Grolman W, Klis SFL. Effects of electrical stimulation on the acoustically evoked auditory-nerve response in guinea pigs with a high-frequency hearing loss. *Hear Res* 2011;272:95–110. [PubMed: 21044671]
24. Choudhury B, Adunka OF, Demason CE, Ahmad FI, Buchman CA, Fitzpatrick DC. Detection of intracochlear damage with cochlear implantation in a gerbil model of hearing loss. *Otol Neurotol* 2011;32:1370–1378. [PubMed: 21921858]

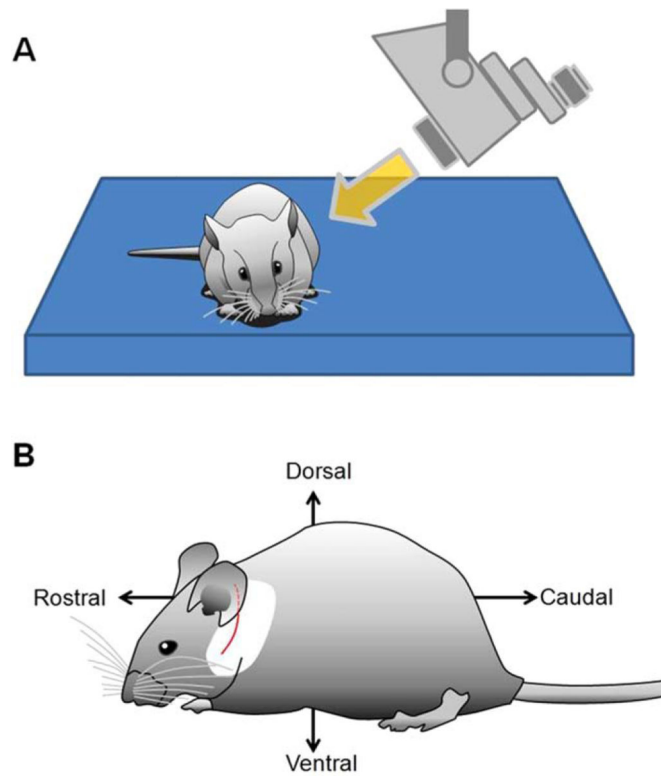


Fig. 1. Preparation of the animal before surgery. (A) The ideal position is prone in accordance with normal body posture of the mouse. (B) Positional descriptions and the 10- to 12-mm modified postauricular skin incision line are shown (red).

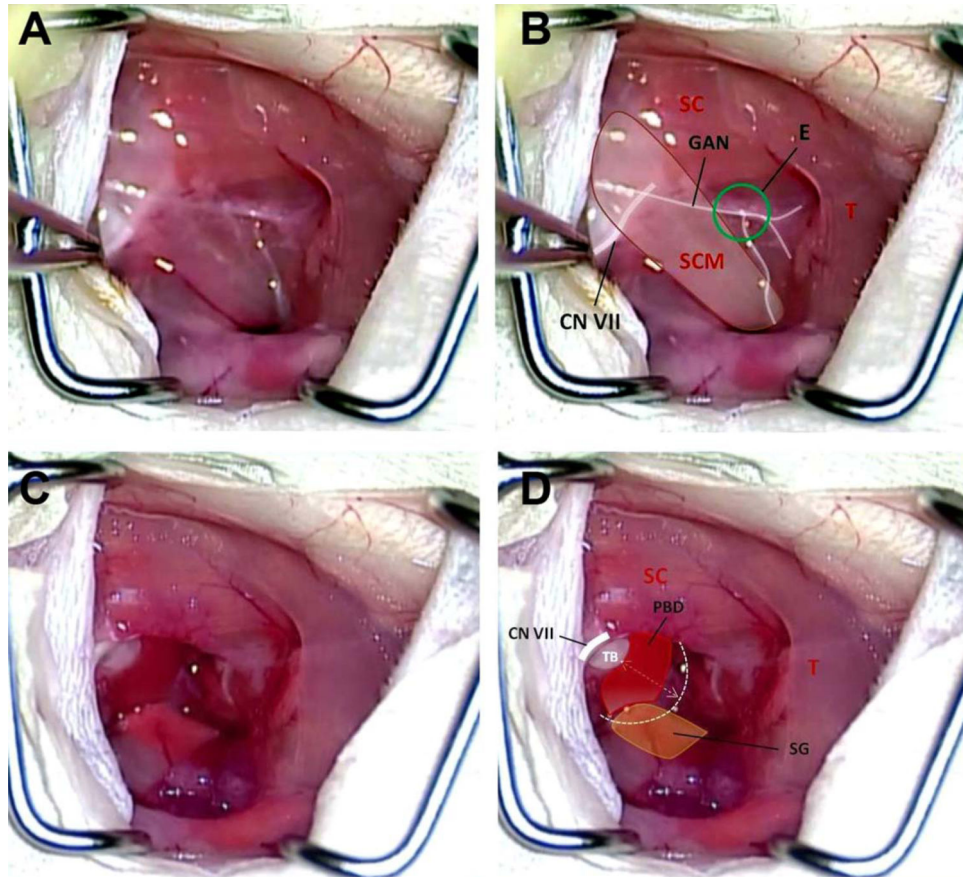


Fig. 2.

(A, B) The surgical anatomy of the neck after the skin incision and retraction of underlying fibromuscular tissue. CN VII = facial nerve; E = Erb's point; GAN = greater auricular nerve; SC = splenius capitis muscle; SCM = sternocleidomastoid muscle; T = trapezius muscle. (C, D) The GAN, SCM, and anterior scalene muscle have been divided, exposing the proximal extratemporal portion of CN VII. This dissection reveals the PBD. PBD = posterior belly of digastrics muscle; SG = submandibular gland; T = trapezius muscle; TB = tympanic bulla.

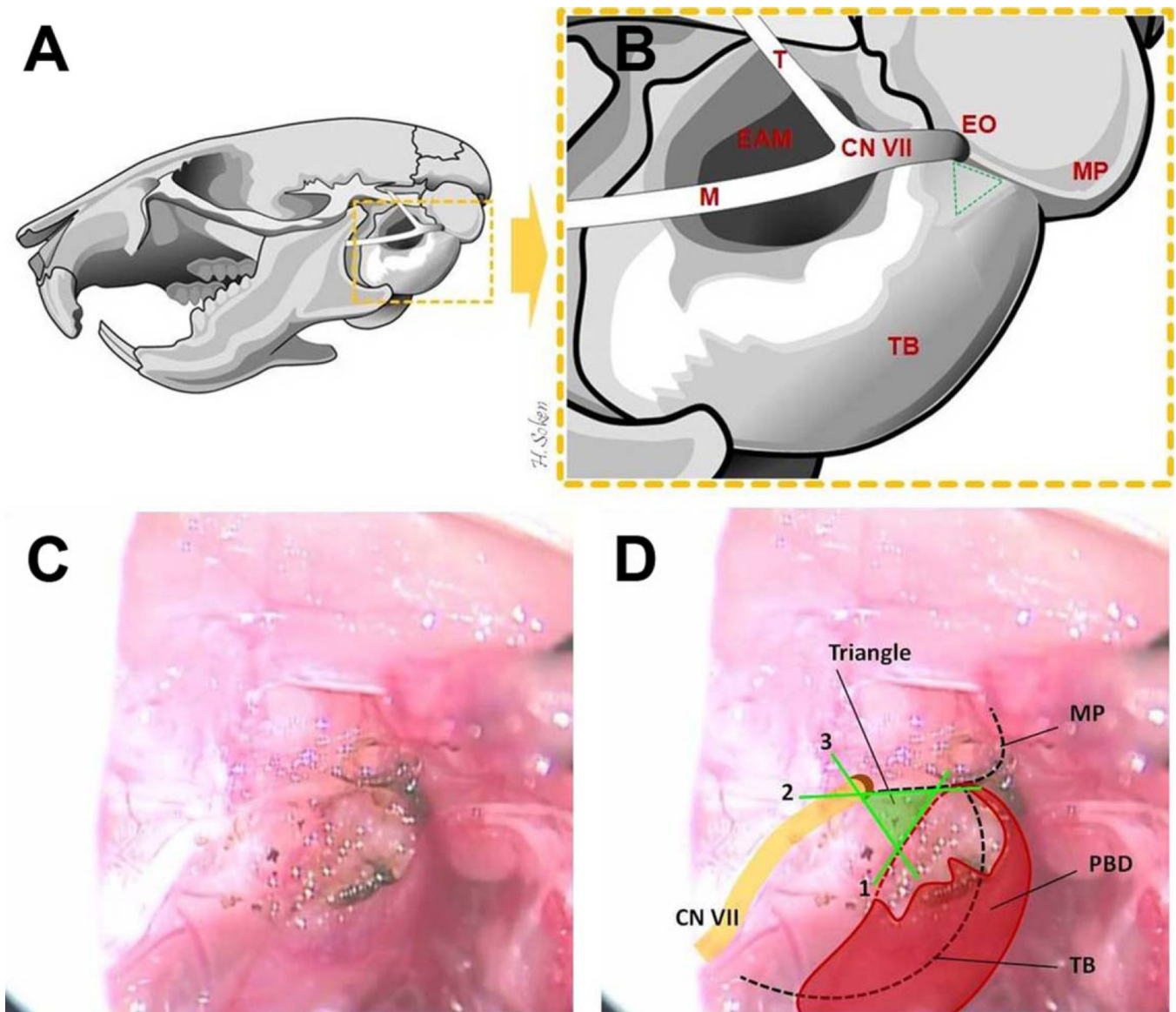


Fig. 3. Temporal bone anatomy and the key landmarks for placement of the tympanotomy. (A, B) The left mouse temporal bone, lateral view, is illustrated. EAM = external acoustic meatus; EO = external orifice of facial nerve (stylomastoid foramen); M = mandibular branch of the facial nerve; MP = mastoid process; T = temporalis branch of the facial nerve; TB = tympanic bulla. (B, C, D) The lines forming the “Tympanotomy Triangle” are both illustrated and depicted in vivo as follows: (1) anterior border of the PBD insertion and/or its bony ridge (digastric ridge), (2) the fissure between TB and MP (tympanomastoid fissure), (3) the line joining the two by crossing the EO (stylomastoid foramen). PBD = posterior belly of digastrics muscle.

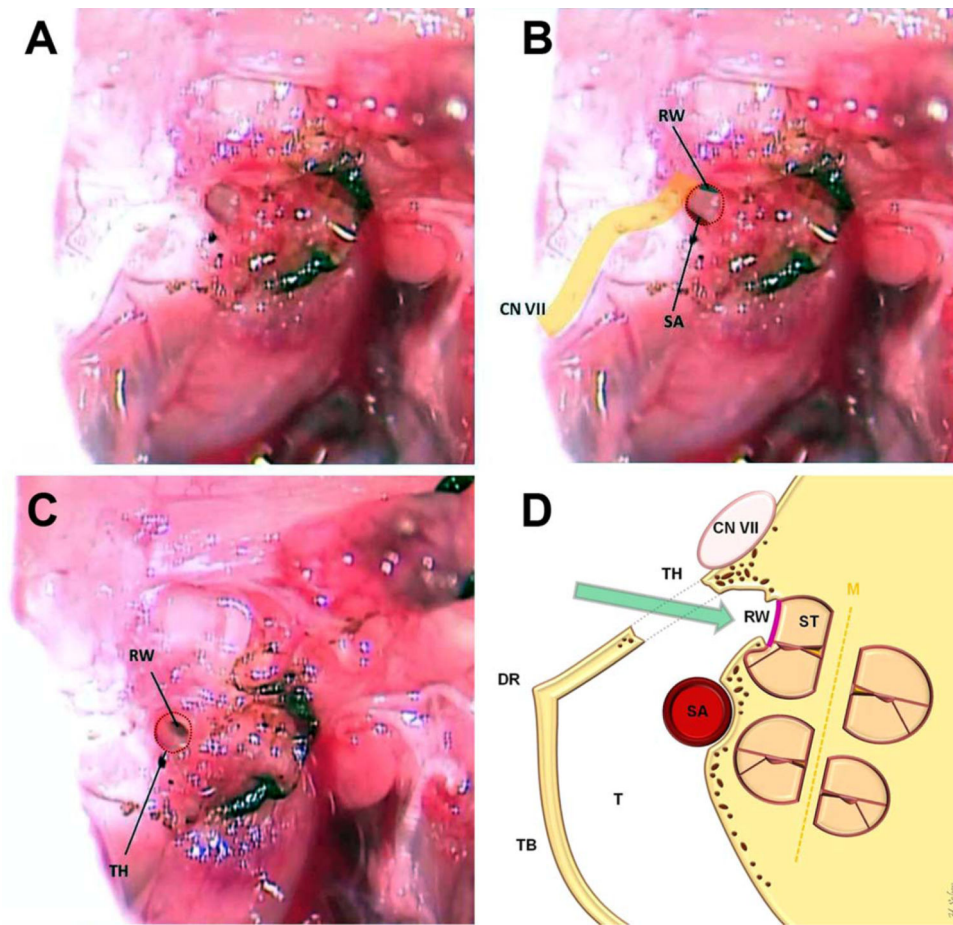


Fig. 4. Access to the middle ear from our tympanotomy hole is shown (A, B). The inferior margin of RW and superior margin of SA are clearly visible. (C) The final view of the tympanotomy hole when complete and ready for RW implantation. (D) The coronal illustration of the cochlea and surgical preparation. CN VII = facial nerve; DR = digastric ridge; M = modiolus; RW = round window; SA = stapedial artery; ST = scala tympani; T = tympanum; TB = tympanic bulla; TH = tympanotomy hole.

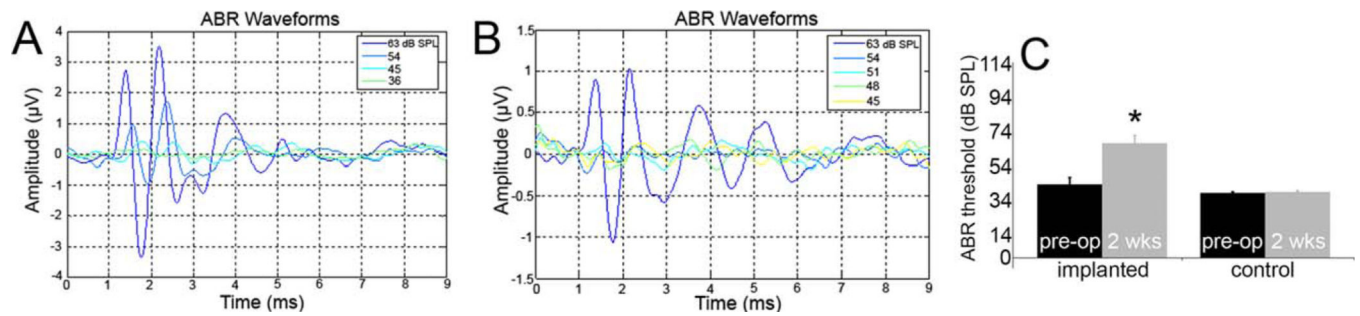


Fig. 5.

Example of typical auditory brainstem response (ABR) recordings. (A) Baseline ABR recording. Threshold was determined to be 36 dB SPL. There are typically five distinct waves between 1 and 6 milliseconds. (B) Example of 2 weeks postoperative ABR recording. Threshold was determined to be 48 dB SPL. (C) Preservation of ABR responses 2 weeks following round-window electrode implantation. Substantial residual hearing is preserved. Nonetheless, the mean implanted ear threshold is significantly higher than the mean preoperative threshold and the mean threshold in the contralateral ears ($*P < .01$, analysis of variance with post hoc Kruskal-Wallis analysis).

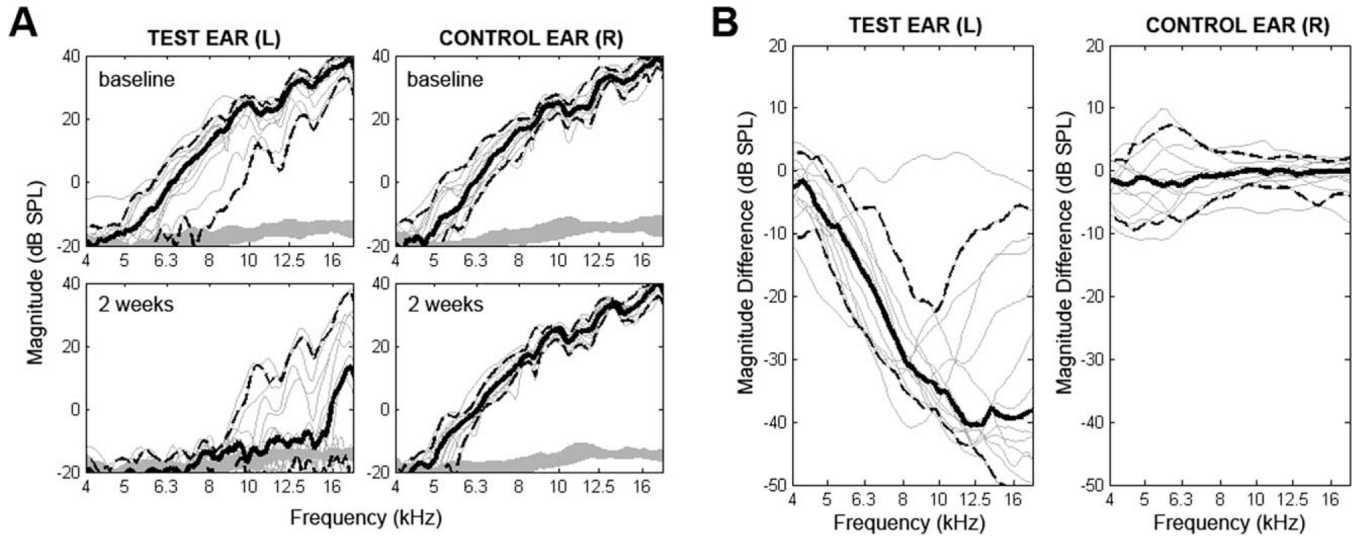


Fig. 6.

Pre- and postoperative distortion product otoacoustic emissions (DPOAE) results for test and contralateral ears. Plots show $2f_1 - f_2$ DPOAE magnitude (dB SPL) as a function of f_2 frequency. Each thin line represents one subject. Solid bold lines represent subject averages in each condition with 95% confidence interval indicated by dashed lines. (A) Baseline and 2-week data are depicted. For the left implanted ear, amplitude of response decreased for every subject. Nine of 15 retained measurable responses above the noise floor. (B) The difference in DPOAE magnitude is plotted for each subject. For frequencies with a large preoperative signal-to-noise ratio, large decreases in magnitude of emissions are seen. Again, outer hair cell function is measurable in nine of 15 subjects. Minimal changes are seen in the contralateral ear.